ELSEVIER

Journal of Alloys and Compounds 446–447 (2007) 248–254

Journal of ALLOYS AND COMPOUNDS

www.elsevier.com/locate/jallcom

Ultrasmall-angle X-ray scattering (USAXS) studies of morphological trends in high energy milled $NaAlH_4$ powders

Tabbetha A. Dobbins [a,b,*], Edward L. Bruster [a], Ejiroghene U. Oteri [a], Jan Ilavsky [c]

[a] *Institute for Micromanufacturing, Louisiana Tech University, P.O. Box 10137, Ruston, LA 71272, United States*
[b] *Department of Physics, Grambling State University, Grambling, LA 71245, United States*
[c] *Advanced Photon Source, Sector 33, Argonne National Laboratory, Argonne, IL 60439, United States*

Received 30 October 2006; received in revised form 18 February 2007; accepted 20 February 2007
Available online 12 March 2007

Abstract

Transition metal dopants added to complex metal hydrides, specifically to sodium aluminum hydride ($NaAlH_4$), by high energy ball milling enhances dehydrogenation kinetics and induces dehydrogenation reaction reversibility. This study uses the power-law scattering parameter, p, gained from ultrasmall-angle X-ray scattering (USAXS) data to elucidate differences in $NaAlH_4$ particle morphology as dopant type and mill time is varied. Four dopant types were used. Two dopant types were used to represent the best kinetic enhancements having high desorption rates (e.g. $TiCl_2$, $TiCl_3$) and were compared with two dopant types which do not perform as well (e.g. $ZrCl_3$ and VCl_3). USAXS data for the doped hydrides were compared with undoped and milled $NaAlH_4$ powders. Mill times used were 0 min (blended), 1, 5, and 25 min. As indicated by the USAXS power-law scattering data, the undoped $NaAlH_4$ powders are comprised of primary particles each having a high surface area. The high particle surface area in the undoped $NaAlH_4$ particle system persists as mill time increases—with only the 25 min sample undergoing a marked a decrease in primary particle surface area. Alternatively, the doped powders milled for 1, 5, and 25 min show uniformly decreasing hydride particle surface area. These decreases in particle surface area may be explained by either the colloidal particles increasing in surface smoothness or decreasing internal void space. $TiCl_3$-doped $NaAlH_4$ powders show the trend of maintaining particles having a morphology comprised of higher particle surface area during the high energy milling stage of powder processing compared with other dopants.

Keywords: Metal hydrides; Ultrasmall-angle X-ray scattering (USAXS); High energy ball milling

1. Introduction

Since the discovery of catalytic effects in transition metal doped sodium alanate ($NaAlH_4$) powders by Bogdanovic and Schwickardi [1], dopant effects in these powders has been studied in an effort to understand and optimize doping strategies to control kinetic barriers to hydrogen release from alanate powders [2–9]. X-ray absorption spectroscopy has been used to characterize the local environment of dopant cations in efforts to elucidate dopant effects [2–9]. In addition to understanding chemical effects of dopants, understanding the effect of the doping process on powder morphology, specifically, controlling powder particle surface area, may be one key aspect which could lead to better control of dehydriding kinetic performance in these systems.

High energy ball milling is typically used to introduce MCl_x catalytic dopants – where M = transition metals such as Ti^{2+}, Ti^{3+}, V^{3+}, and Zr^{4+} – into sodium alanate ($NaAlH_4$) powders. However, high energy ball milling both with and without dopant additions, is known to have pronounced effects on powder particle morphology. Such change in powder morphology, when studied by scanning electron microscopy, is not easily tractable due to the stochastic nature of the high energy milling process. Decrease in powder particle size is expected to occur during the high energy milling process. Typically, decreasing particle size results in an increase in powder surface area per unit volume. Additionally, surface area changes occurring in each alanate powder particle (i.e. porous or rough particles versus smooth

* Corresponding author at: Institute for Micromanufacturing, Louisiana Tech University, P.O. Box 10137, Ruston, LA 71272, United States.
Tel.: +1 318 257 5134; fax: +1 318 257 5104.
E-mail address: tdobbins@latech.edu (T.A. Dobbins).

0925-8388/$ – see front matter © 2007 Elsevier B.V. All rights reserved.
doi:10.1016/j.jallcom.2007.02.161

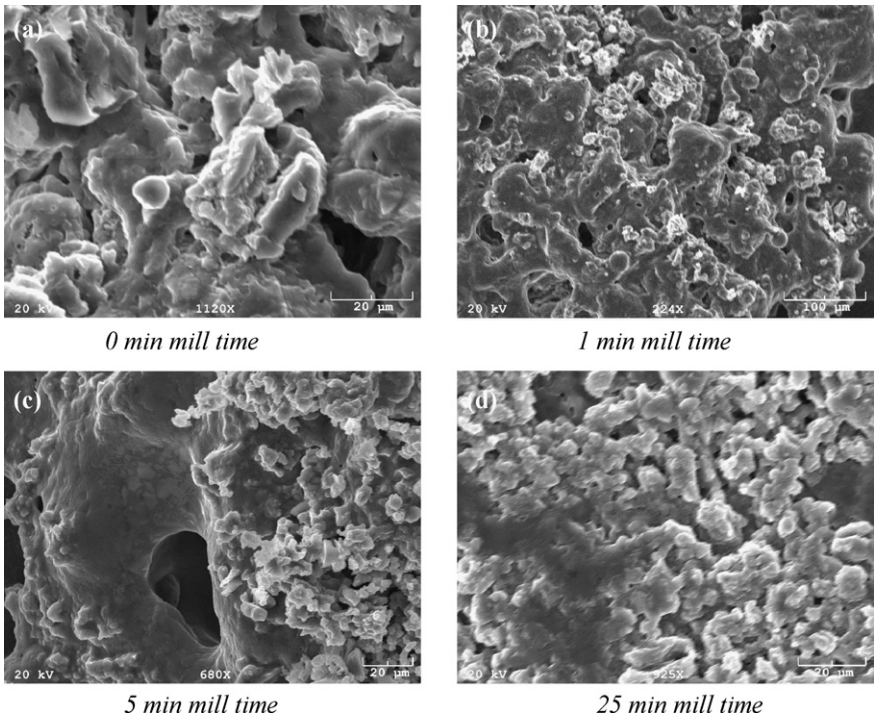

Fig. 1. SEM images of the surface of an undoped $NaAlH_4$ powder particle blended for 2 min in dry N_2 glovebox and milled for (a) 0 min; (b) 1 min; (c) 5 min; (d) 25 min.

particle surfaces) will also affect the efficiency of the gas/solid desorption reaction occurring at the hydride particle surface,

$$NaAlH_4 \Leftrightarrow (1/3)Na_3AlH_6 + (2/3)Al + H_2$$
$$\Leftrightarrow NaH + Al + (3/2)H_2$$

Ultrasmall-angle X-ray scattering (USAXS) makes possible the parameterization of colloidal particle systems using the surface fractal dimension (D_s) extracted from the power-law scattering regime of intensity (I) versus scattering wave vector ($\mathbf{Q}$) scattering data, where $|\mathbf{Q}| = (4\pi/\lambda)(\sin\theta)$ and 2θ is scattering angle [10–15]. Power-law scattering data from surface fractals (i.e. dense colloidal particles having a high surface area contributed by either surface roughness or by internal particle void space) are characterized by log $|I|$ versus log$|\mathbf{Q}|$ slopes (*called power-law slope, p*) between −3 and −4 [15]. These power-law slopes are related to powder particle surface area, S, through the parameter surface fractal dimension, D_s—whereby $D_s = p + 2D$ (with D being mass fractal dimension and $D = 3$ for colloidal particles). The surface fractal dimension, D_s, relates powder particle surface area to particle size R by the relationship: $S \sim R^{D_s}$. For rough particles the parameter, D_s, varies between 2 and 3 (D_s approaches 3 for high surface area particles). By this formalism, colloidal particles having a low surface area (i.e. smooth particles with no internal voids) are characterized by the measured power-law slope $p = -4$ and those having high surface area (i.e. rough particles having internal voids) are characterized by $p = -3$ [15].

Electron microscopy of sodium alanate powders reveals primary particle structures which have both high surface roughness (i.e. each particle is comprised of a set of smaller particles) and internal void space (i.e. each particle is not a fully dense colloid). Understanding those particle morphologies using only scanning electron microscopy is challenging—particularly when the most valuable contribution of morphological studies is made when those morphologies are well enough characterized to track the behavior of the powder system as milling occurs or as dopant type is varied. Parameterization of USAXS data into power-law slope (p) enables the effects of dopant type, concentration, and mill time on powder morphology to be tracked. It bears noting that USAXS data is collected from a statistically significant

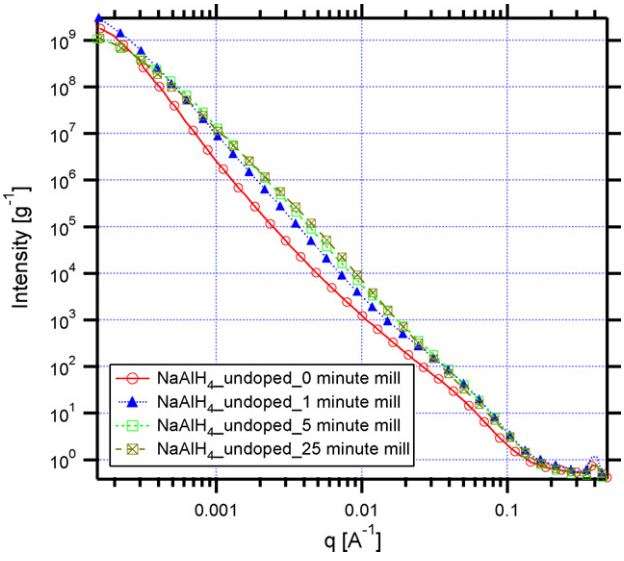

Fig. 2. USAXS data: undoped $NaAlH_4$ powders blended for 2 min in dry N_2 glovebox and milled for (a) 0 min; (b) 1 min; (c) 5 min; (d) 25 min.

population of powder particles (on the order of mg of powder is contained in each measurement).

2. Experimental

2.1. Materials preparation

Commercial sodium alanate powders ($NaAlH_4$) (Sigma–Aldrich Corp.) was blended with 2 mol% each of $TiCl_2$, VCl_3, and $ZrCl_4$ and with 4 mol% each of $TiCl_2$ and $TiCl_3$. The dopant powders were purchased from Sigma–Aldrich Corp. Samples were blended under a dry N_2 glovebox environment using an agate mortar and pestle for 2 min and subsequently milled (Certiprep SPEX 8000M high energy mill) using a tungsten carbide vial containing 3 g of WC milling media for times of 1, 5, and 25 min. For USAXS measurement, the milled powders were sealed between 3 mm thick kapton films. Some of the milled powders were reserved for scanning electron microscopy (AMRAY 1830 scanning electron microscope). For reference, undoped $NaAlH_4$ powders were blended, milled and prepared for USAXS and SEM analysis.

2.2. Ultrasmall-angle X-ray scattering (USAXS)

Ultrasmall-angle X-ray scattering (USAXS) uses single crystal optics to extend the dynamic **Q**-vector range to lower values compared to standard SAXS instruments and makes it possible to measure features above 1 μm in size [10–12]. Using 1D-collimated USAXS instrument (with only vertically collimating crystals) the data are slit smeared. Numerical desmearing routines are available for isotropic microstructures—yielding pin-hole collimated USAXS data [13,14]. While it is possible to fit power-law scattering to slit-smeared data and correctly obtain the fractal dimension, this can be done reliably only for data at Q values significantly lower than slit length; or data at Q values significantly higher than slit length, when the data are effectively 2D colimated even when Bonse–Hart geometry is used. However, around slit length (around 0.04 $Å^{-1}$ for current experiment) the data transition from slit smeared into 2D collimated geometries and fractal dimension cannot be established by simple fitting of the power-law slope to the data. While it is possible to develop analytical fitting function which accounts for slit smearing and slit length, we opted to first desmear the data using well established and tested method used routinely and reliably at the USAXS instrument and then power-law can be fitted anywhere in the whole Q range to establish fractal dimension [12]. We have verified on selected data sets, that when selected fitted Q range is reliably within slit-smeared Q range (for $Q \ll$ slit length) the fractal dimensions are (within fitting errors) the same as when fitted to desmeared data. Absolute calibration of the intensity versus **Q**-vector data makes USAXS viable for yielding scattered intensity data normalized per gram of powder.

USAXS data were collected at Sector 33ID at the Advanced Photon Source, Argonne National Laboratory (Argonne, IL) using an X-ray energy of 11 keV. The USAXS instrument has a large dynamic **Q** range in slit-smeared configura-

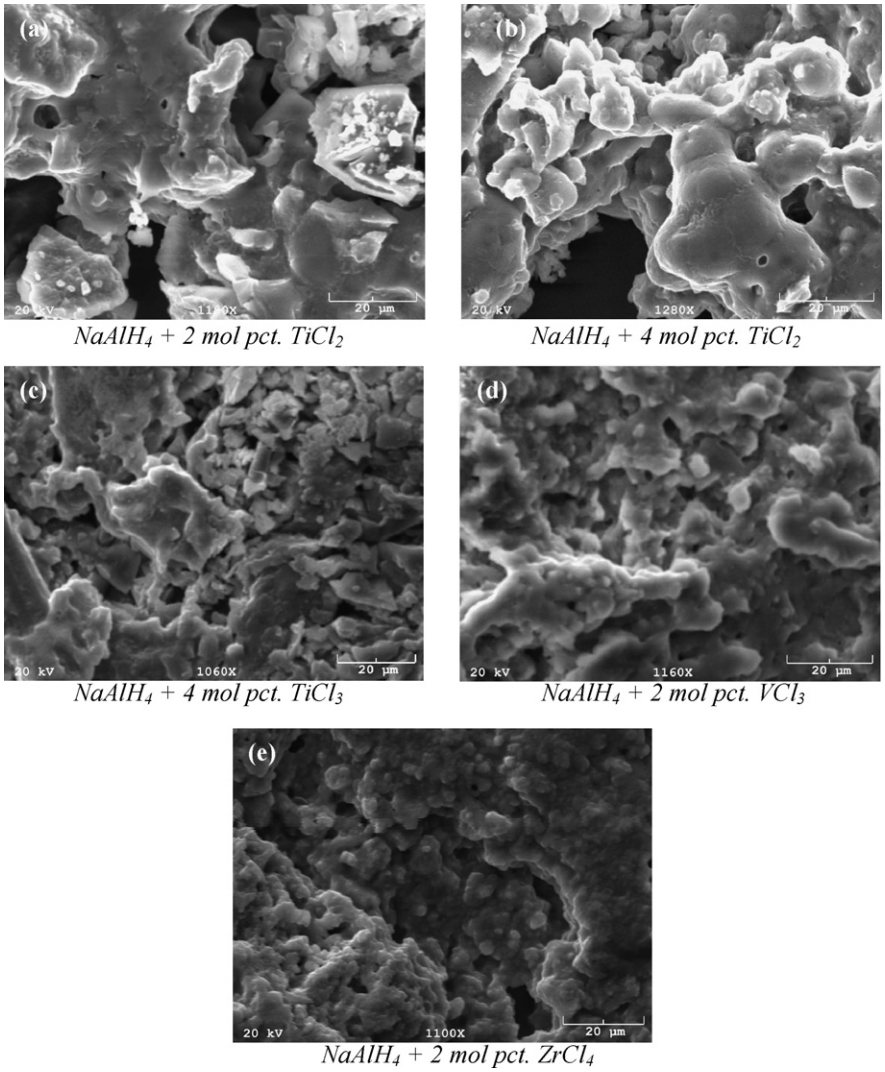

Fig. 3. SEM images of $M^{x+}Cl_x$-doped $NaAlH_4$ powders milled for 1 min where M^{x+} is (a) 2 mol% $TiCl_2$; (b) 4 mol% $TiCl_2$; (c) 4 mol% $TiCl_3$; (d) 2 mol% VCl_3 and 2 mol% $ZrCl_4$.

tion (1.5×10^{-4} Å^{-1} < |**Q**| < 1 Å^{-1}). The USAXS data is measured with a high **Q** resolution of ~1.5×10^{-4} Å^{-1}. Data reduction and analysis routines were performed with IGOR PRO 5.0.3 using Irena version 1 and Indra version 2 subroutines [13,14]. The absolute intensity calibration of the data was corrected for multiple scattering where observed. Multiple scattering influences data at low Q values and with intensities close to peak values. Observed peak broadening (expressed as FWHM) in the current experiment were between no broadening (no multiple scattering) and up to three times broader as compared to empty beam peak profile. Therefore the data below $Q \sim 10^{-3}$ Å^{-1} (which generally represents over two decades of intensity from the peak value) were not used for establishing the fractal dimension. This minimizes the chance that the data in tables are contaminated by multiple scattering.

3. Results and discussion

3.1. Morphology of undoped sodium alanate ($NaAlH_4$) powders

The complex particle morphology of undoped $NaAlH_4$ powders can be seen in the scanning electron microscopy images of Fig. 1 showing high magnification images of powder particle surfaces before milling (Fig. 1(a)) and after milling for 1 min (Fig. 1(b)), 5 min (Fig. 1(c)), and 25 min (Fig. 1(d)). Both before and after milling, the powder particle is comprised of high surface roughness and internal porosity—both factors contribute to high particle surface area. Clear delineation of, and comparisons among, these complex microstructures is not achievable using SEM images alone. The USAXS data shown in Fig. 2 were obtained from undoped $NaAlH_4$ powders. USAXS power-law slopes, p, were measured from the scattering curves in the Q-range from 0.0035 to 0.016 Å^{-1}. For the various mill times of 0, 1, 5, and 25 min, the USAXS power-law slope, p, is given by −3.00, −3.34, −3.29, and −3.55 indicating colloidal particles with a rough surface (or spongy porous particles containing internal pores or groves) for the p near to −3.0 and lower particle surface area as p approaches −4. High energy milling has the effect of decreasing surface area of colloidal $NaAlH_4$ particles. For chemically homogeneous distribution of the dopant species, milling for times between 5 and 25 min are needed.

The as-purchased $NaAlH_4$ powders are comprised of small colloidal particles corresponding to a Guinnier region having a radius of gyration of around $2\pi/Q = 21$ nm [10]. These particles disappear from the microstructure – either by attaching to larger particles or fusing together – during high energy milling. With respect to the particle surface roughness obtained using USAXS power-law slope, p, the undoped $NaAlH_4$ powders are characterized by particles having high surface roughness—indicated by a USAXS power-law slope, p, between at nearly −3 (for the unmilled powders). As mill time increases to 1 and 5 min, the USAXS power-law slope, p, approaches −3.33, indicating a structural transition toward powder particles containing less internal surface. At the maximum mill time used for these studies—25 min, the USAXS power-law had a maximum value of −3.55, indicating that $NaAlH_4$ particle morphologies are comprised of colloidal particles containing fewer internal surfaces as a result of high energy milling.

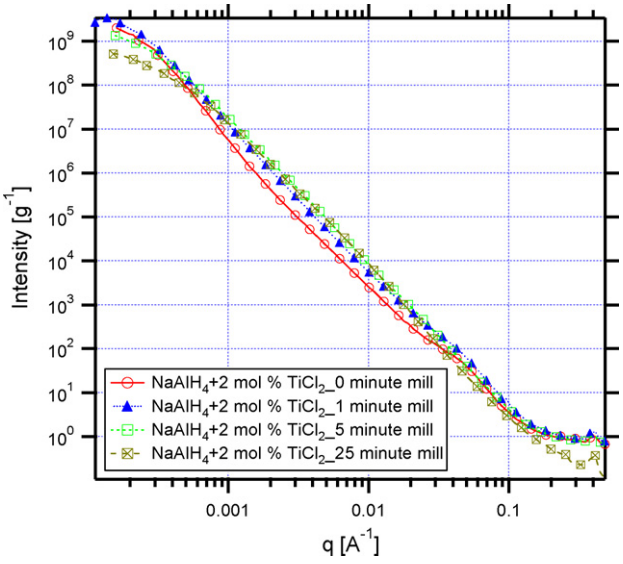

Fig. 4. USAXS data: 2 mol% $TiCl_2$ doped $NaAlH_4$ powders blended for 2 min in dry N_2 glovebox and milled for (a) 0 min; (b) 1 min; (c) 5 min; (d) 25 min.

3.2. Morphology of the y mol% MCl_x-doped $NaAlH_4$ powders

The remainder of this work addresses the variations in USAXS power-law slope, p, as a means for tracking the $NaAlH_4$ particle surface area in the doped sodium alanate systems. Fig. 3 shows SEM of the surface of unmilled $M^{x+}Cl_x$-doped $NaAlH_4$, where $M^{x+} = TiCl_2$, $TiCl_3$, VCl_3, and $ZrCl_4$. In each case, the $NaAlH_4$ particles appear to be comprised of both surface roughness and internal porosity. USAXS data in Figs. 4–6 were collected from 2 mol% $TiCl_2$-doped, 4 mol% $TiCl_2$-doped and 4 mol% $TiCl_3$-doped $NaAlH_4$ powders, respectively. USAXS data in Fig. 7 were collected from 2 mol% VCl_3-doped $NaAlH_4$ powders. USAXS data in Fig. 8 were collected from 2 mol%

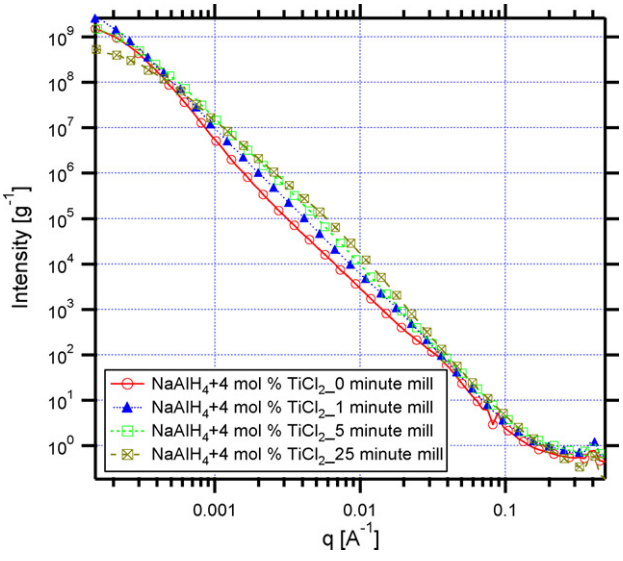

Fig. 5. USAXS data: 4 mol% $TiCl_2$ doped $NaAlH_4$ powders blended for 2 min in dry N_2 glovebox and milled for (a) 0 min; (b) 1 min; (c) 5 min; (d) 25 min.

Table 1
USAXS power-law (p) given by the slope of log (I) vs. log(**Q**) or I–Q^p

USAXS power-law exponent (p)	$NaAlH_4$	$NaAlH_4$ + 2 mol% $TiCl_2$	$NaAlH_4$ + 4 mol% $TiCl_2$	$NaAlH_4$ + 4 mol% $TiCl_3$	$NaAlH_4$ + 2 mol% VCl_3	$NaAlH_4$ + 2 mol% $ZrCl_4$
0 min mill	−3.00	−3.10	−3.07	−3. 38	−3.23	−3.33
1 min mill	−3.34	−3.26	−3.15	−3.14	−3.22	−3.22
5 min mill	−3.29	−3.38	−3.43	−3.18	−3.40	−3.43
25 min mill	−3.55	−3.45	−3.29	−3.57	−3.45	−3.30

Power-law slope behavior yields particle morphology information. For rough colloids the power-law slope, p, has values between −3 and −4 (p closer to −4 for smooth colloids and p closer to −3 for rough colloids). Variance was less than ±0.024.

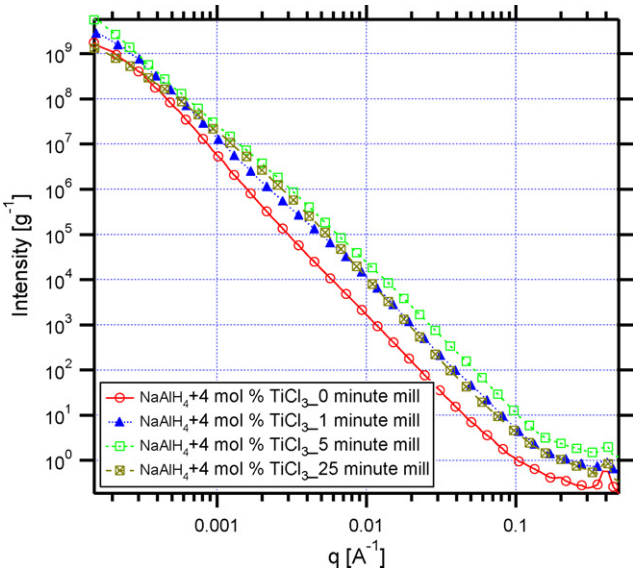

Fig. 6. USAXS data: 4 mol% $TiCl_3$-doped $NaAlH_4$ powders blended for 2 min in dry N_2 glovebox and milled for (a) 0 min; (b) 1 min; (c) 5 min; (d) 25 min.

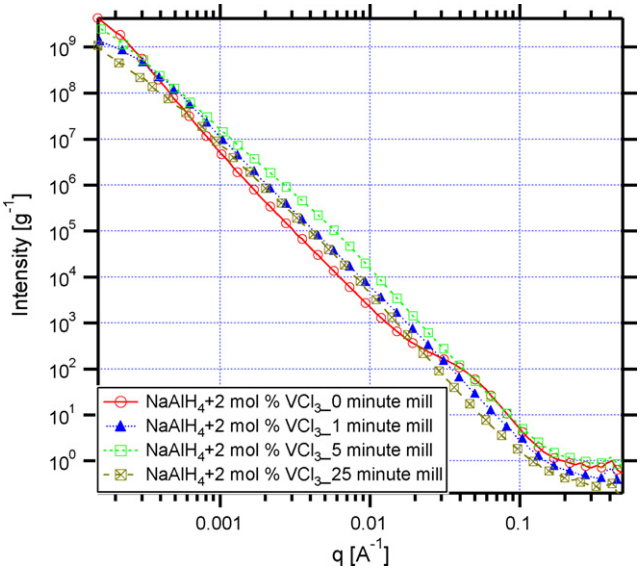

Fig. 7. USAXS data: 2 mol% VCl_3 doped $NaAlH_4$ powders blended for 2 min in dry N_2 glovebox and milled for (a) 0 min; (b) 1 min; (c) 5 min; (d) 25 min.

$ZrCl_4$-doped $NaAlH_4$ powders. For each of the USAXS curves, power-law slopes, p, were measured from the scattering curves in the Q-range from 0.0035 to 0.016 Å^{-1}. The USAXS power-law slopes, p, measured from undoped and doped $NaAlH_4$ powders are presented in Table 1.

USAXS data reveals that key trends exist between alanate particle morphology, powder milling time and dopant type. Fig. 9(a)–(c) contains the absolute value of USAXS power-law slope, $|p|$, data versus mill time for each powder system studied. Compared with the undoped $NaAlH_4$ system, all MCl_x dopant systems led to an average lower surface area for the colloidal particles comprising the system immediately following dopant additions for the unmilled powders (as indicated by a higher $|p|$ in Fig. 9). The initial increase in $|p|$ is possibly due to the addition of smooth colloidal dopant particles. After 1 min mill time, the undoped $NaAlH_4$ powders measured higher values of $|p|$ than the doped powders for each dopant type. This indicates that the early stage of doping results in an increase powder particle surface area, possibly due to porosity introduced by dopant assisted desorption H_2 gases. The highest dopant content—i.e. 4 mol% $TiCl_2$ dopant and 4 mol% $TiCl_3$ realized the lowest value of $|p|$ corresponding to the highest average particle surface area. After

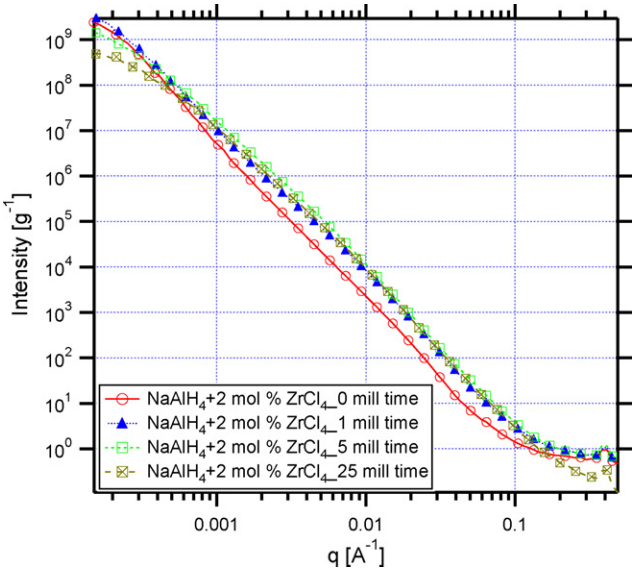

Fig. 8. USAXS data: 2 mol% $ZrCl_4$ doped $NaAlH_4$ powders blended for 2 min in dry N_2 glovebox and milled for (a) 0 min; (b) 1 min; (c) 5 min; (d) 25 min.

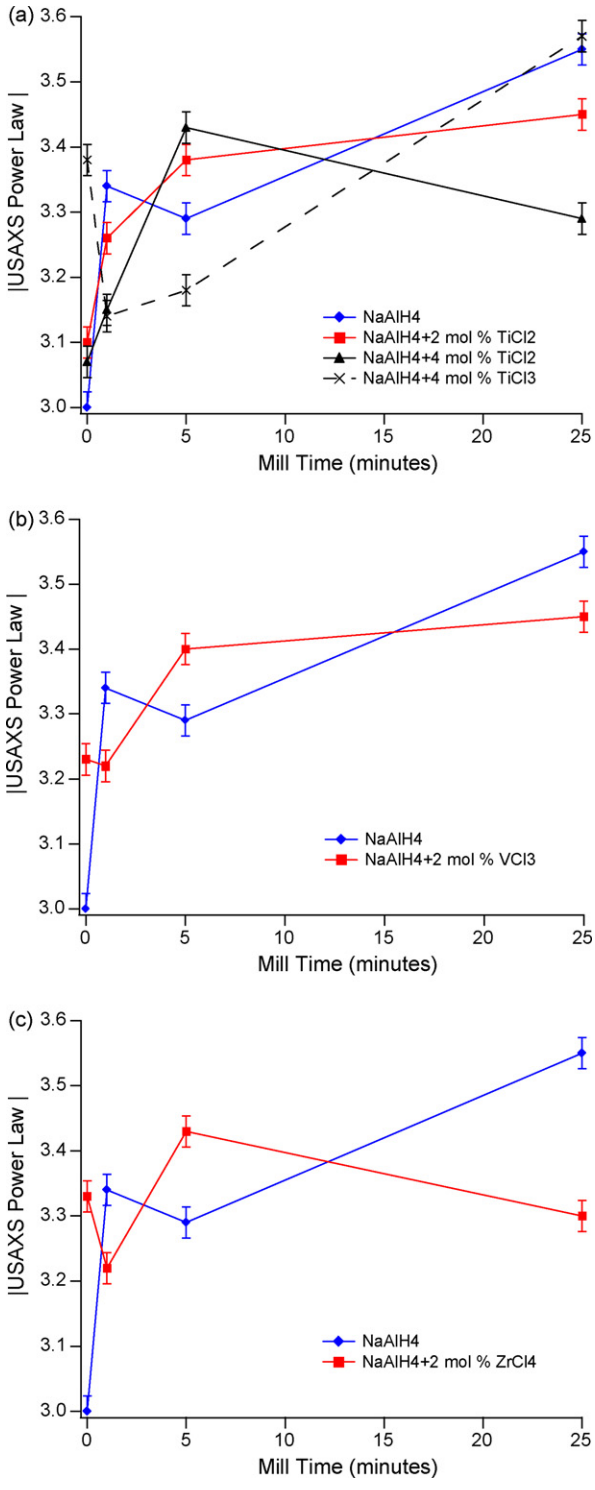

Fig. 9. USAXS power-law slopes, p, for the $M^{x+}Cl_x$-doped $NaAlH_4$ powders (a) the $Ti^{x+}Cl_x$-dopants; (b) 2 mol% VCl_3-dopant; (c) 2 mol% $ZrCl_4$-dopant. The 4 mol% $TiCl_3$-doped NaAlH4 powders have the lowest surface area during high energy milling times up to approximately 15 min.

5 min mill time, the each doped $NaAlH_4$ powder system was comprised of particles each having a higher average surface area than the undoped powders milled for 5 min —with the exception of $TiCl_3$. The $TiCl_3$-doped $NaAlH_4$ powders realized very high surface area for each colloidal particle for much longer mill times (excess of 5 min). Anton provided kinetic performance data for the dopants investigated in the form of desorption rate after 5 min of desorption time: $TiCl_3$ (6.57 wt.%/h), $TiCl_2$ (3.98 wt.%/h), VCl_3 (1.80 wt.%/h), and $ZrCl_4$ (1.50 wt.%/h) [2]. It may be concluded that the ability for the powder to homogeneously distribute the MCl_x dopant species in order for it to chemically catalyze the H_2 desorption reaction, while maintaining a low $|p|$ (rougher particle surface) may be a key indicator dopant kinetic performance.

4. Conclusions

USAXS data has provided a practical approach to parameterize stochastic microstructures produces during high energy ball milling of doped and undoped $NaAlH_4$ powders. This approach could be applied to a wide variety of hydrogen storage materials in efforts to correlate processing, de/rehydrogenation, and doping effects on powder morphology. Here, USAXS data parameterized, using surface fractal analysis, shows that doped alanate powders decrease particle surface roughness with longer mill times. Compared to other dopants, $TiCl_3$ provides a highest powder particle surface area—corresponding to the lowest value of $|p|$ for 1 and 5 min mill times (and linearly extrapolated up to 15 min mill time as shown in Fig. 9(a). Since 5 min mill processing is expected to produce homogeneous distribution of dopant, it is concluded that the best dopants will maintain rougher colloidal hydride particle surfaces during homogeneous dopant distribution.

Acknowledgments

Funding for this project was provided by the Department of Energy, Office of Basic Energy Sciences (Contract No.: DE-FG02-05ER46246). Use of the Advanced Photon Source was supported by the U.S. Department of Energy, Office of Science, Office of Basic Energy Sciences, under Contract No. W-31-109-ENG-38.

References

[1] B. Bogdanovic, M. Schwickardi, J. Alloys Compd. 253–254 (1997) 1–9.
[2] D.L. Anton, J. Alloys Compd. 356 (2003) 400–404.
[3] J. Graetz, J.J. Reilly, J. Johnson, A. Ignatov, A. Yu, T.A. Tyson, Appl. Phys. Lett. 85 (2004) 500–502.
[4] A. Leon, O. Kircher, H. Rosner, B. Decamps, E. Leroy, M. Fichtner, A. Percheron-Guegan, J. Alloys Compd. 414 (2006) 190–203.
[5] A. Leon, J. Rothe, O. Kircher, M. Fichtner, J. Phys. Chem. B 108 (2004) 16372–16376.
[6] A. Leon, R.J. Schild, M. Fichtner, Chem. Eng. Trans. 8 (2005) 171–176.
[7] A. Leon, O. Kircher, M. Fichtner, J. Rothe, J. Phys. Chem. B 110 (2006) 1192–1200.
[8] E. Bruster, T.A. Dobbins, R. Tittsworth, D.L. Anton, Mater. Res. Soc. Symp. Proc. 837 (2005), N3.4.1.
[9] T.A. Dobbins, R. Tittsworth, S.A. Speakman, J. Schneibel, in: D. Chandra, J.J. Petrovic, R. Bautista, A. Imam (Eds.), A Symposium in Honor of Drs. Gary Sandrock, Louis Schlapbach, and Seijirau Suda, 2006, pp. 263–270.

[10] J. Ilavsky, A.J. Allen, G.G. Long, P.R. Jemian, Rev. Sci. Instrum. 73 (2002) 1660–1662.
[11] G.G. Long, A.J. Allen, J. Ilavsky, P.R. Jemian, P. Zschack, in: P. Pianetta, J. Arthur, S. Brennan (Eds.), SRI99: Eleventh U.S. National Synchrotron Radiation Instrumentation Conference, AIP Conference Proceedings CP521, American Institute of Physics, New York, 2000, pp. 183–187.
[12] G.G. Long, P.R. Jemian, J.R. Weertman, D.R. Black, H.E. Burdette, R. Spal, J. Appl. Cryst. 24 (1991) 30–37.
[13] Indra 2 Homepage. http://www.uni.aps.anl.gov/%7Eilavsky/indra_2.html.
[14] Irena 2 package of SAS data evaluation and modeling macros for Igor Pro Homepage. http://www.uni.aps.anl.gov/%7Eilavsky/irena.html.
[15] D.W. Schaefer, Science 243 (1989) 1023–1027.